Measurement of chain tilt angle in fully hydrated bilayers of gel phase lecithins

S. Tristram-Nagle,* R. Zhang,‡ R. M. Suter,‡ C. R. Worthington,* W.-J. Sun,‡ and J. F. Nagle*‡
*Departments of Biological Sciences and ‡Physics, Carnegie Mellon University, Pittsburgh, Pennsylvania 15213 USA

ABSTRACT The tilt angle θ_{tilt} of the hydrocarbon chains has been determined for the fully hydrated gel phase of a series of saturated lecithins. Oriented samples were prepared on glass substrates and hydrated with supersaturated water vapor. Evidence for full hydration was the same intensity pattern of the low angle lamellar peaks and the same lamellar repeat D as unoriented multilamellar vesicles. Tilting the sample permitted observation of all the wide angle arcs necessary to verify the theoretical diffraction pattern corresponding to tilting of the chains towards nearest neighbors. The length of the scattering unit corresponds to two hydrocarbon chains, requiring each bilayer to scatter coherently rather than each monolayer. For DPPC, θ_{tilt} was determined to be 32.0 ± 0.5° at 19°C, slightly larger than previous direct determinations and considerably smaller than the value required by recent gravimetric measurements. This new value allows more accurate determinations of a variety of structural parameters, such as area per lipid molecule, A = 47.2 ± 0.5 Å^2, and number of water molecules of hydration, n_w = 11.8 ± 0.7.

As the chain length n of the lipids was increased from 16 to 20 carbons, the parameters A and n_w remained constant, suggesting that the headgroup packing is at its excluded volume limit for this range. However, θ_{tilt} increased by 3° and the chain area A_c decreased by 0.5 Å^2. This behavior is explained in terms of a competition between a bulk free energy term and a finite or end effect term.

INTRODUCTION

Quantitative measurements of lipid bilayer structure provide fundamental data for discussion of biomembrane structure and function. Although many structural studies of lipid bilayers have been reported, at the present time there is considerable disagreement even for the most studied lipid, namely dipalmitoylphosphatidylcholine (DPPC). For the most biologically relevant L_α phase of DPPC, literature values for A, the area per lipid in the plane perpendicular to the bilayer normal, range from 58 Å^2 to 71 Å^2 (30, 44). Since A for the gel phase of DPPC is at least 44 Å^2, this means that the uncertainty of the effect of melting the hydrocarbon chains is at the 100% level (14 Å^2 versus 27 Å^2 for ΔA).

This paper focuses on the fully hydrated $L_{\beta'}$ gel phase of DPPC. One rationale is that the better ordered gel phase enables a more complete and accurate structural determination which may then be used to test various methods for application to the L_α phase. That this is not an idle exercise is illustrated by the disagreement in A in the gel phase obtained using the following two methods. One of these methods is the gravimetric/hydration method (5, 15, 16, 17, 22, 34, 36, 43) which measures the lamellar spacing D as a function of water content to obtain the number n_w of water molecules/lipid above which D remains constant. Then n_w is used in the following equation, which is equivalent to one introduced by Luzzati (23),

$$A = 2(V_L + n_w V_w)/D, \quad (1)$$

along with measured values (1, 19, 31, 35, 49) of the lipid volume V_L and the volume of water V_W, to obtain A. For the gel phase another method for obtaining A uses the equation

$$A = 2A_c/\cos\theta_{tilt}, \quad (2)$$

where θ_{tilt} is the tilt angle of the hydrocarbon chains and A_c is the area/chain measured perpendicularly to the long axis of the chains; Eq. 2 applies to lipids with two chains/lipid. The area A_c has been routinely measured using x-ray diffraction in fully hydrated unoriented MLV dispersions (9, 21, 24, 34, 43). In Fig. 1 measurements of θ_{tilt} as a function of A and n_w are shown. There is a major disagreement in Fig. 1 in that all previous measurements of θ_{tilt} give lower values for A, by ~7 Å^2, when compared to the latest results from the gravimetric/hydration method (22, 34). When one considers that the minimum packing of crystalline hydrocarbon chains near 20°C is ~38 Å^2/pair of chains (39), this yields nearly 100% error in determining the effect of forming a hydrated gel phase (8 Å^2 versus 15 Å^2 for ΔA). This discrepancy is of more general concern than just the gel phase of DPPC since many of the values of A given in the literature for L_α phases of many lipids have been obtained solely using the gravimetric method.

In a previous paper (48) it was argued that the measurements of θ_{tilt} gave more consistent results for A and that the intrinsic uncertainties in the placement of water in defect regions in unoriented MLVs would explain why measurements of n_w are too large, leading to values of A from Eq. 1 that are too large. However, we have still been concerned that the measurements of θ_{tilt} may have been consistently too small for the following reasons. Levine (20) prepared oriented DPPC bilayers on a teflon substrate and obtained θ_{tilt} = 28°, but his geometry cut off equatorial scattering. Levine's interpretation of hydrocarbon chain packing was criticized by Stamatoff et al. (42) who did not observe the necessary equatorial scattering, even though it was permitted by their geome-

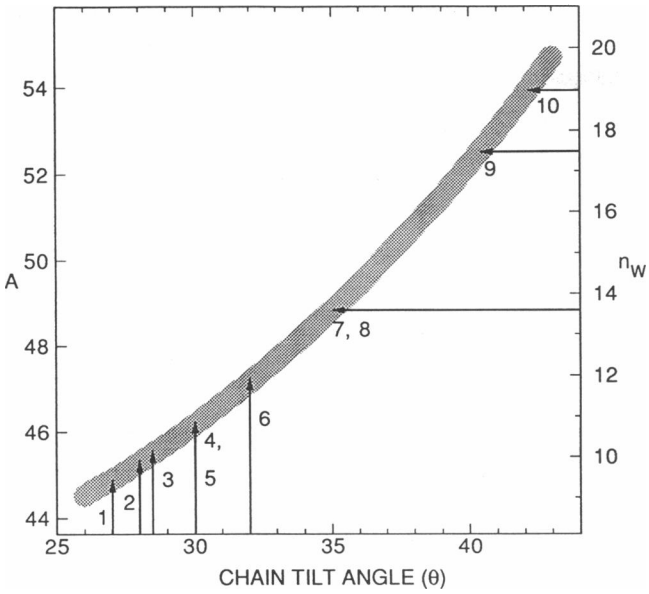

FIGURE 1 Relation between θ_{tilt} (°), A (Å^2) and n_w from Eqs. 1 and 2 is indicated by the gray curve for $DC_{16}PC$. The center of the gray curve uses our current values at 19°C and the width of the gray curve uses our current errors in V_L (0.9358 ± 0.002 ml/g), D (63.4 ± 0.1 Å), and A_c (20.0 ± 0.1 Å^2). Vertical arrows indicate determinations of θ_{tilt} and horizontal arrows indicate determinations of n_w. The numbers on the arrows indicate the work of the following references: **1** (reference 3); **2** (reference 21); **3** (12); **4** (41); **5** (24); **6** (this work); **7** (17); **8** (43); **9** (22); **10** (34).

try. The best resolved data (41) have been obtained for free-standing films of DMPC for which θ_{tilt} was accurately measured to be 30°. The concern here is that the sample is compressed by the free water/air boundary and that this compression in turn affects the structure of the individual bilayers. This is suggested by earlier results that θ_{tilt} (43) and the continuous scattering transform vary with hydration (45), and reports that the bilayer thickness changes with hydration (18, 22, 43). This concern is reinforced by the fact that D for free standing films is 6 Å less than for fully hydrated MLVs (40). This amount of compression in D is comparable to the difference between fully hydrated and dry bilayers (45). Hentshel and Rustichelli (12) recently obtained θ_{tilt} = 28.5°, but for D,L-DPPC bilayers instead of L-α-DPPC, and it is not clear that their samples were fully hydrated. Buldt et al. (2) stated that their results were compatible with the value θ_{tilt} = 32° ascribed to Tardieu et al. (43), but straightforward calculation of θ_{tilt} from their positions of the C4 and C15 carbons yields θ_{tilt} = 27–28°. However, their D of 62.5 Å (2) and n_w = 13.6 might be criticized as indicating less than full hydration when compared to later gravimetric results (34, 22). McIntosh (24) employed an indirect method involving some plausible assumptions in comparing DPPE and DPPC to obtain θ_{tilt} equal to 30°.

The first goal in this paper is to determine θ_{tilt} accurately and directly for fully hydrated gel phase L-α-DPPC. The approach taken will be to study oriented bilayers on a solid substrate. Although preparation of oriented samples for resonance studies has been routine for many years, it is not so easy to fully hydrate oriented bilayers in a geometry suitable for diffraction studies. Criteria to be met for full hydration of the oriented bilayers are that they have (*a*) the same D and (*b*) the same intensity pattern of the lamellar reflections as ordinary fully hydrated unoriented dispersions. A criterion to be met by x-ray diffraction is that all wide-angle peaks be observable in order to establish the chain packing that is assumed in the equations that determine θ_{tilt}. The second goal of this paper is to study the chain length dependence of lipid packing in lecithin bilayers, particularly θ_{tilt}, A, A_c, D, and n_w. A preliminary report of this research has been given (46).

MATERIALS AND METHODS

Lipids. Synthetic lecithins (1,2-diacyl-*sn*-glycero-3-phosphatidylcholine) (39) were purchased from Avanti Polar Lipids (Birmingham, AL) and used without further purification. The two fatty acid chains were identical, linear and saturated, each with n carbons. In this study n was varied from 16 to 20. The abbreviation DC_nPC will be used; e.g., DPPC will also be called $DC_{16}PC$. The high purity of these lipids was indicated by the sharp main transitions of fully hydrated dispersions obtained with an MC-1 calorimeter (MicroCal, Inc., Amherst, MA). When scanned at 10°C/h, the full widths at half maximum height were: 0.11°C for $DC_{16}PC$, 0.09°C for $DC_{17}PC$, 0.13°C for $DC_{18}PC$, 0.11°C for $DC_{19}PC$, and 0.14°C for $DC_{20}PC$.

Oriented bilayers. Thin 00 glass coverslips (Biophysica Technologies, Baltimore, MD), 3 cm × 3 cm × 70 μm, were cleaned by soaking and swabbing with HPLC grade chloroform (Aldrich, Milwaukee, WI). Dry lipid (5–10 mg) was dissolved in 200 μl chloroform/methanol (3–4.5 to 1, vol/vol, with the lower part of the range preferred for larger n) and the entire solution was then applied to the coverslip. During initial evaporation of the solvent, constant rocking of the coverslip (supported by a glass slide), rolling the lipid solution back and forth to the edges of the coverslip, enhanced orientation of the bilayers. Orientation of the bilayers parallel to the coverslip was also enhanced by a final 24-h air drying at 5°C. Visualization of the 5–10 μm thick sample (~1,000 bilayers) by polarized light microscopy provided preliminary indication of successful orientation; bilayers that were well oriented, as later verified by x-ray diffraction, appeared as dark uniform fields under crossed polars. With too much methanol in the solvent surface defects that looked like "crosses" formed and with too much chloroform deeper defect structures formed that looked like "curls." Successful preparation of oriented bilayers may involve an equal rate of evaporation of chloroform and methanol from the bilayers, which is affected by temperature and humidity of the room, chain length, and concentration of lipid. The organic solvents were allowed to evaporate at least for several days at room temperature and then the coverslip with oriented bilayers was cut to obtain an 8 mm × 3 cm sample strip. Storage of these samples at room temperature for several months caused no degradation of the lipid as determined by thin layer chromatography (chloroform:methanol:water, 60:30:5).

A sample chamber, shown in Fig. 2, was machined from a block of solid aluminum. A trough in the center of the chamber was filled with deionized, purified water, and a removable cover had thin (1.5 μm) mylar windows (Dupont, Wilmington, DE) to allow passage of x-rays. A Peltier cooler (1.5 × 3 × 0.36 cm high) (model CP 1.0-63-06L; Melcor Thermoelectrics, Trenton, NJ) was mounted with the cooling side facing up on top of each of the two posts. The ends of the sample strip were glued to these two coolers.

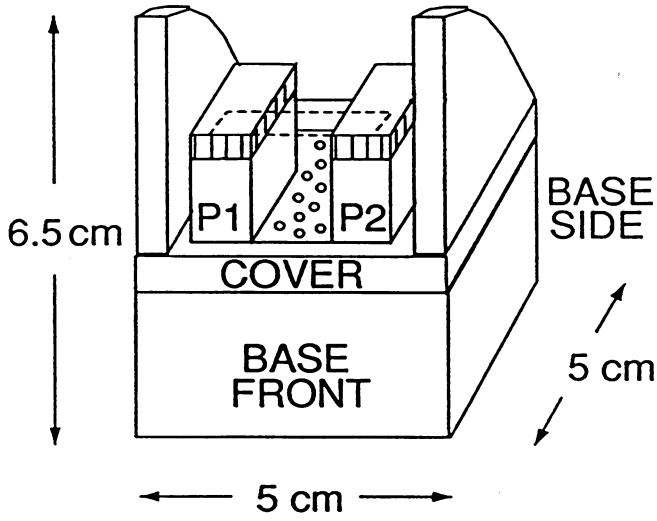

FIGURE 2 The hydration chamber for oriented bilayers. The base contains a trough for water (*circles*) and two posts (*P1* and *P2*). On top of each post is a Peltier cooler. The coverslip position is shown in dashed lines and the oriented lipid bilayers are on the top of the coverslip facing away from the Peltier coolers. A large wrap-around mylar window (not shown), glued over the top of the solid cover support shown, permits detection of wide angle diffraction at both the beam geometries indicated in Fig. 3.

Hydration of the oriented bilayers was achieved in the sealed sample chamber. First, the chamber with sample was placed into an oven at 70–80°C and allowed to equilibrate for 1 h. As is well known, lipids will not become fully hydrated from water vapor even at 100% relative humidity (40, 45, 47, 33). To circumvent this vapor pressure paradox, the Peltier coolers were turned on so that the coverslip was slightly cooler than the water vapor (<1°C difference measured on the surface of the coverslip). This caused water to condense gently from the vapor onto the oriented bilayers. Too much condensation created a water layer that was too thick and disrupted the orientation of the lipid films. Too little condensation led to incomplete hydration. Results will be given for two hydration conditions, *H1* and *H2*. For *H1*, which yields less than fully hydrated samples, 30–40 milliamps of current were applied for 1 h; for *H2*, which yields fully hydrated samples, 40–50 milliamps of current were applied for 4–6 h. The window of current and time that gave sufficient water condensation for full hydration of the lipid without flooding the sample was quite small. Times of 8 h at 80°C did not significantly degrade the sample as determined by thin layer chromatography, since the amount of lysolecithin formed was estimated to be <0.1%. After hydration the Peltier coolers were turned off, the sample chamber was removed from the oven, allowed to cool to the desired temperature, and mounted in the x-ray beam. Even the presence of bulk water in the sample chamber trough, maintaining 100% relative humidity in the chamber, did not suffice to prevent the eventual reduction of the *d*-spacing from the value for fully hydrated bilayers. However, this dehydration was sufficiently slow that diffraction data could be obtained in more hydrated states. Although most of the data for θ_{tilt} in oriented samples were obtained at room temperature (~25°C), there is a small temperature dependence in the tilt angle which was finally checked while controlling the chamber temperature to 19 ± 1°C.

Unoriented bilayers. Multilamellar vesicles (MLVs) were prepared by adding 25 mg of lipid to 75 mg of deionized distilled water, and cycling the dispersion three times between 90 and 5°C with 5 min of vortexing at each temperature. When such dispersions are made up with excess water, they settle into a clear solvent layer on top and an opaque layer on bottom containing multilamellar vesicles; the dividing line gradually moves down the tube over periods of weeks. Thin walled 1.0 mm glass x-ray capillaries (Charles Supper Co.) were cleaned by sequentially washing with a chromic acid bath, deionized water, acetone, and finally copious amounts of deionized water. After drying with nitrogen the capillaries were flame sealed at one end. The MLV dispersion was then loaded into the capillaries using a 1.0 ml Hamilton syringe. In order to remove air bubbles, the capillaries were centrifuged for 10 min at 1,100 *g* at room temperature. This amount of centrifugation did not overly compress the lipid, since upon standing for one week at atmospheric pressure, the lipid settled even further; in addition the low angle *D* spacing was the same with and without centrifugation. After centrifugation the capillaries were flame-sealed above the water layer, and this seal was dipped in Duco cement. Upon completion of the diffraction experiments, it was confirmed that the samples had remained fully hydrated by observing the presence of the excess water layer above the opaque lipid dispersion.

X-ray diffraction. The x-ray source was an Elliot rotating anode Type GX21, typically run at 5.3 kW. For unoriented samples a graphite monochromator selected Cu K_α radiation (λ = 1.5418 Å) and defined a beam with angular resolution $\delta(2\theta)$ (HWHM) = 0.04° in the horizontal direction, with horizontal dimension 0.4 mm and with vertical dimension defined by slits to be 3 mm. A Braun (Munich, Germany) position sensitive detector (PSD) with an effective linear resolution of 0.2 mm was placed 57.2 cm in the horizontal direction from the sample. Evacuated flight paths contained the main beam and the scattered x-rays.

The axis of the lipid capillary was held vertically in a chamber machined from aluminum with mylar windows (different from the one in Fig. 2). A calibrated silicon diode (Type DT-470-CU-13) coated with Dow Corning heat sink compound (Midland, MI) was seated in a pocket in the aluminum block next to the capillary. The diode was connected to a Lake Shore Cryotronics (Westerville, OH) model DRC 84C temperature controller which monitored the temperature and controlled two thermofoil heating strips (Minco Products, Minneapolis, MN) on either side of the aluminum block at 19 ± 1°C. The temperature at the capillary was found to be 1° higher than the temperature in the sample chamber in a separate experiment using a miniature thin film detector (model TFD; Omega Engineering, Stamford, CT) that was glued to the capillary and had been precalibrated to the above silicon diode.

For oriented samples the x-ray beam was passed through a nickel filter to remove Cu K_β radiation and was collimated with a simple pinhole collimator (0.3 mm holes 6.5 cm apart) and the data were recorded on Kodak DEF5 x-ray film (Charles Supper Co., Natick, MA). The hydration chamber shown in Fig. 2 was placed into the beam in one of two positions differing by the angle ω between the coverslip and the beam, as indicated in Fig. 3. For small values of ω, nominally 5° as indicated in Fig. 3 *A*, the sample was first exposed with the film holder in position s_1. Then the same film was moved in its holder to position s_2 without moving the sample and the distance s_2–s_1 was accurately established (13.46 cm). The rationale for the use of two *s* distances is to obtain a more accurate determination of the lamellar *D* spacing as explained in the results section. Notice in Fig. 3 *B* that for larger ω, nominally 45°, the x-ray beam first passes through the coverslip and then through the sample. This eliminates the artifact of differential absorption by the glass of x-rays scattered in different directions by the sample. Total sequential x-ray exposure times were typically 3 hours at both large and small ω (1 h at s_1 and 2 h at s_2).

Neutral density centrifugation. This technique is described in reference 49 and involves hydrating lipid in 3 ml of a mixture of H_2O and D_2O (Aldrich Chemical Co., Inc., Milwaukee, WI) to produce the desired absolute specific density in 3 ml plastic, screw-top tubes. Centrifugation was carried out at 1,100 *g* for 1 h. The temperature was held at 19 ± 0.2°C by placing the centrifuge in a refrigerated chamber containing a heater controlled by a YSI Proportional Temperature Controller model 72 (Yellow Springs, OH). After centrifugation the temperature

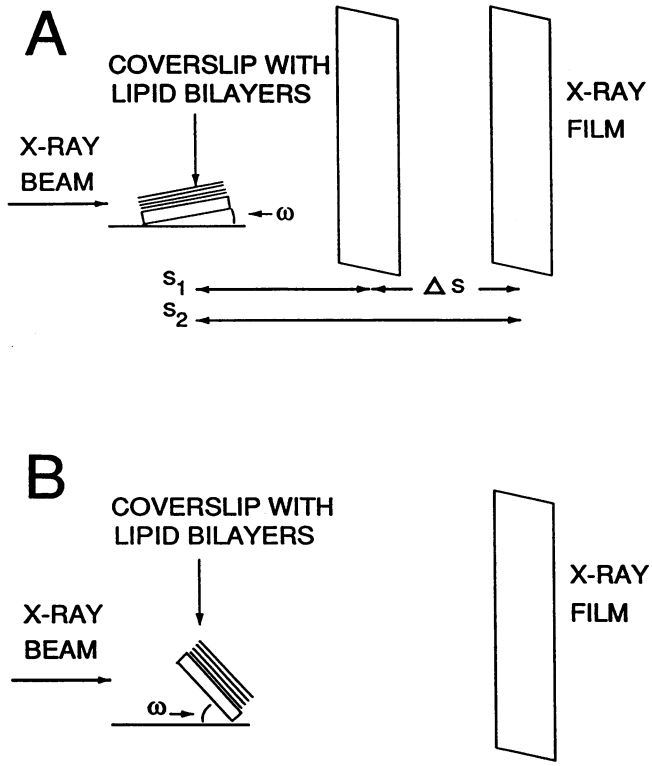

FIGURE 3 (*A*) Geometry for small angle of incidence, ω. The rationale for two sample to film distances, s_1 and s_2, is given in the results section. (*B*) Geometry for large angle of incidence, ω. For both geometries the chamber in Fig. 2 was positioned so that its side planes were parallel to the x-ray beam.

was checked by rapidly inserting a precalibrated thermistor probe into a control tube in one of the centrifuge buckets.

THEORY

Conformationally ordered hydrocarbon chains pack together in a nearly hexagonal lattice, but with deviations consistent with orthorhombic (face-centered rectangular) symmetry. Although the chains could *a priori* be tilted in various directions relative to this packing pattern (11, 12, 14, 41), it has been known for a long time (20) (and will be confirmed by the results in this paper) that the fully hydrated gel phase of DPPC is characterized by the chains being tilted in the direction towards nearest neighboring chains. Also, each bilayer scatters independently in the wide angle region due to lack of registry of individual molecules across the aqueous spaces (20, 43). In this case the main features of the **q**-space wide angle pattern of a single bilayer of perfectly ordered tilted molecules are shown in Fig. 4. The scattering is confined to Bragg rods; the observable ones with highest intensity are the 20 and 11 rods. The peak intensity along the 20 rods occurs on the equator ($q_z = 0$), corresponding to in-plane scattering, whereas the peak intensity along the 11 rods is centered at symmetrically equivalent nonzero values of q_z.

The spacings d_{11} and d_{20} corresponding to the positions of peak intensity along the 11 and 20 rods are slightly different due to small deviations from hexagonal symmetry. The area per chain A_c in a plane perpendicular to the chains (which is necessarily tilted by θ_{tilt} from the plane of the bilayer) is given by

$$A_c = \frac{d_{20}d_{11}}{\sqrt{1 - (d_{11}/2d_{20})^2}}. \quad (3)$$

Also, θ_{tilt} is simply related to the **q**-space geometry by

$$\sin(\theta_{tilt}) = \frac{\sin(\hat{\theta})}{\sqrt{1 - (d_{11}/2d_{20})^2}}, \quad (4)$$

where $\hat{\theta}$ is exactly the angle in **q**-space to the center of the 11 peak if the hydrocarbon chains are lines of delta functions. We have performed calculations (not presented) for more realistic models (14) of the hydrocarbon chains which show that the displacement of the angle of the maximum scattering along the 11 Bragg rod is less than 0.1°.

The laboratory geometry that is theoretically simplest and most often employed aligns the x-ray beam nearly parallel to the plane of the bilayers. Then, the wide-angle scattering pattern on the x-ray film is very similar to the **q**-space pattern in Fig. 4. However, even a thin solid substrate absorbs most of the x-rays scattered through it. Also, scattering in the plane of the bilayer is especially strongly absorbed by the bilayers themselves. In practice, therefore, only the upper pair of the 11 peaks in Fig. 4 is clearly observed in this laboratory geometry. The other

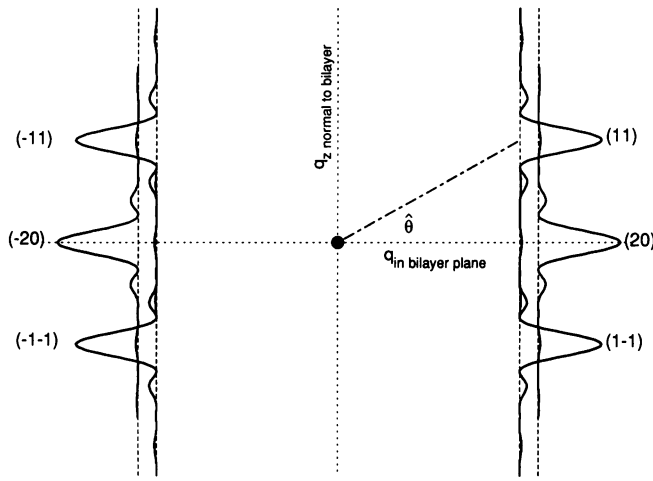

FIGURE 4 The *q*-space pattern for a nearly hexagonal array of chains of length L tilted toward nearest neighbors. The origin is indicated by the solid circle, the vertical axis is for the component of **q** normal to the bilayer and the horizontal axis is for all components of **q** in the plane of the bilayer. The location of the Bragg rods are shown as vertical dashed lines. The intensities along these rods are shown as the horizontal distances between the solid curves and their underlying dashed lines. For the simplest model of thin chains these intensities are sinc functions. The angle $\hat{\theta}$ appears in Eq. 4.

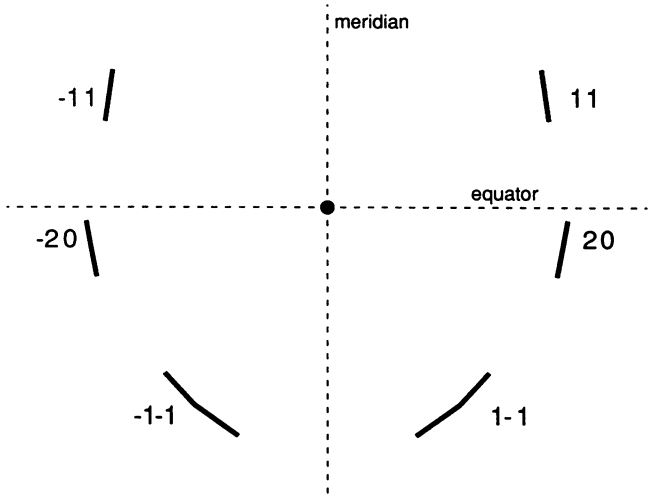

FIGURE 5 The calculated film pattern for $\omega = 45°$ that corresponds to the $(\pm 2, 0)$ and $(\pm 1, \pm 1)$ central peaks in the q-space pattern in Fig. 4.

simple geometry is for the beam to be perpendicular to the bilayers, but this only yields powder averaged diffraction rings since the bilayers are rotationally (about the bilayer normal) unoriented with respect to each other.

In order to verify that the samples conform to the theoretical pattern in Fig. 4, one must consider other geometries in which all the arcs can be observed. The only other geometry that can be considered involves tilting the oriented bilayers at an angle ω with respect to the beam about an axis that is parallel to the equator on the x-ray film, as shown in Fig. 3 *B*. Let the position on an x-ray film be described by its Bragg angle θ (determined by distance from the center of the film) and the angle η measured from the equator. Then, for elastic scattering, the corresponding point in **q**-space is given by

$$q_z = k[\sin(2\theta)\sin(\eta)\cos(\omega) + (1 - \cos(2\theta))\sin(\omega)] \quad (5)$$

and

$$q_{in} = [4k^2 \sin^2\theta - q_z^2]^{1/2},$$

where $k = 2\pi/\lambda$, q_{in} is the in-plane scattering vector which is the horizontal axis in Fig. 4 and q_z is the component of θ normal to the plane of the bilayer which is the vertical axis in Fig. 4. These equations can also be inverted to calculate the film pattern that would be observed for the **q**-space pattern in Fig. 4. Fig. 5 shows such a calculated pattern for $\omega = 45°$, $\theta_{tilt} = 31.5°$ and with an effective chain length, $L = 40$ Å, corresponding to two hydrocarbon chains.

RESULTS

X-ray diffraction patterns for oriented bilayers of $DC_{16}PC$ are shown in Fig. 6 when the x-rays are incident at small angles ω, as shown in Fig. 3 *A*. Most of the x-rays scattered towards the coverslip are absorbed, so the lower part of the film is relatively featureless, with only the main beam and occasionally some of the strongest reflections showing. Scattering down the length of the coverslip is especially strongly absorbed which accounts for the light line that is clearly seen for the s_1 distance. This light line shown by a double arrow in Fig. 6 occurs at the angle ω of tilt of the coverslip; ω was nominally set to 5° and the calculations of ω from this light line are quite close to this. Many orders h of lamellar reflection occur simultaneously on the meridian because the bilayers are not perfectly oriented, and there is a distribution of angles of the normals of the bilayers relative to the normal to the coverslip with a maximum in the distribution at zero relative angle. From the growth of arc lengths with order h, the mosaic spread would be estimated to be at least 3°, and a somewhat larger mosaic spread would be consistent with the number of simultaneously observed orders. Because ω is near 5–7°, the relative intensities of the different orders seen in Fig. 6 are distorted, with orders h = 7–9 being most strongly amplified because their Bragg angles are near ω. Those reflections that lie below the light line include orders h = 1, 2, 3 for the *H1* hydrated sample and orders h = 1–4 for the *H2* hydrated sample. These orders are either not visible (Fig. 6, *H1*) or much weaker (Fig. 6, *H2*) than those that occur above the light line. Although a light line from the coverslip is not apparent for the s_2 distance exposure, the intensity pattern of the orders is the same. Inclusion of the arcs below the light line in the D spacing calculation did not change the result within the error.

For the *H1* sample in Fig. 6 the reflections are identified, in ascending order along the meridian, as follows: a strong 4th order occurs at the edge of the s_1 light line, a strong 5th order, a weak 6th order, a strong 7th order, an 8th order that is barely visible on the original film and a strong 9th order. Further reflections along the meridian are the lamellar orders from the s_2 distance exposure; these reflections are identified by having wider arcs and centers that are slightly offset to the right. They include strong orders h = 4, 5, 7, and 9 with the 6th order barely visible on the film.

For the *H2* sample exposed at s_1, orders 2, 3, and 4 are weakly present below the light line and orders 5, 7, 9, and 10 are strongly present above the light line. This same pattern is also seen for the s_2 exposure, and in addition the $h = -1$ and -2 orders are weakly visible. The absence of h = 6 and h = 8 is characteristic of fully hydrated $DC_{16}PC$.

Calculation of the lamellar spacing D used the reflections from both s_1 and s_2 exposures, since it was easy to measure s_2–s_1 accurately but difficult to measure either s_1 or s_2 accurately due to uncertainty in determining where the x-ray beam intersects the sample when ω is small. Also, it was difficult to measure the center of the main beam accurately enough when the beam stop was

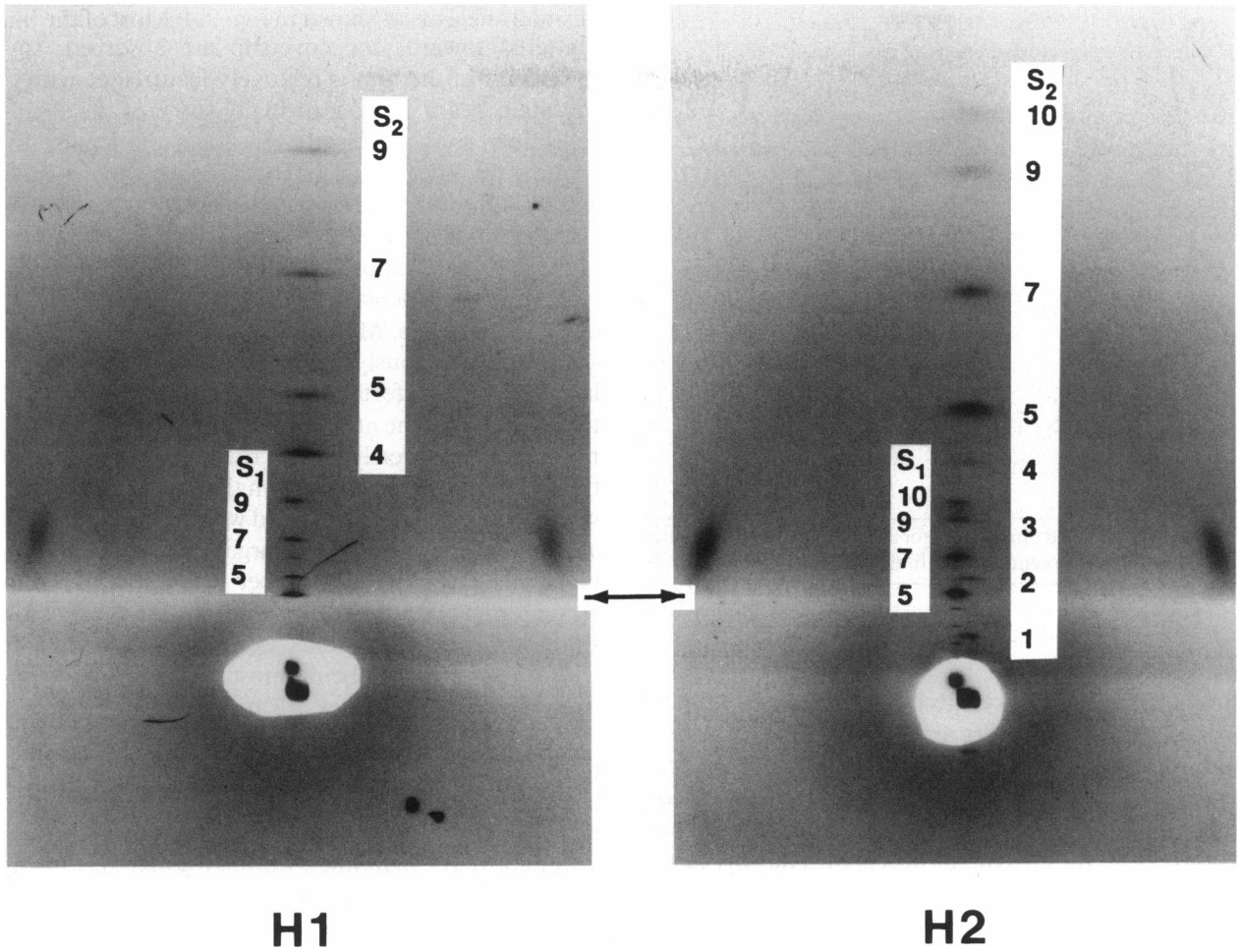

FIGURE 6 Diffraction from oriented bilayers of gel phase $DC_{16}PC$ taken at small angles of incidence, ω. Each film was exposed twice, first at distance s_1 and then at a larger distance s_2. The second exposure, which has the longer arcs and larger beamspot, is shifted slightly to the right from the first exposure. The numbers refer to the order number h, with some visible orders unnumbered due to space limitations. $H1$, partially hydrated sample, with $s_1 = 61.0$ mm, $s_2 = 195.6$ mm, $\omega = 5.3°$, $D = 62.5 \pm 0.2$ Å, and $\theta_{tilt} = 31.6 \pm 0.5°$. $H2$, fully hydrated sample with $s_1 = 58.1$ mm, $s_2 = 192.7$ mm, $\omega = 6.9°$, $D = 63.4 \pm 0.3$ Å, and $\theta_{tilt} = 31.3 \pm 0.5°$. The double arrow indicates the light line discussed in the text. These data were taken at room temperature (25°C).

removed. Therefore, four unknowns, s_1, D, and the two centers, c_1 and c_2, for the main beam, for distances s_1 and s_2, respectively, were determined by minimizing the sum of squares of the deviations of the lamellar reflections from the values given by Bragg's law. Since there were always at least three measured reflections for each of the two values of s, the solution was properly overdetermined and easily solved by a least squares minimization routine in which the values of c_1 and c_2 were constrained to lie within the large main beam spots in Fig. 6 and the value of s_1 was constrained to lie within the maximum and minimum measured distances allowed by the size of the coverslip. Only the indexing of the lamellar reflections given in the preceding paragraphs yielded feasible fits. For the *H1* film in Fig. 6 the resulting value of D was 62.5 ± 0.2 Å, and for the *H2* film in Fig. 6 D was 63.4 ± 0.3 Å.

The films in Fig. 6 also show strong wide angle reflections for the s_1 exposure. For both the *H1* and *H2* hydration conditions the apparent centers of these reflections for the $(1, \pm 1)$ arcs occur at an angle $\eta_{11} = 26.3 \pm 0.3°$ above the equator. To obtain θ_{tilt} the film features were first transformed to **q**-space using Eq. 5 and the measured values of ω to obtain $\hat{\theta}$ which was then used in Eq. 4 to give $\theta_{tilt} = 31.5 \pm 0.5°$. The latter calculation also requires d_{11} and d_{20}, which were measured to high accuracy for unoriented bilayers. Even though d_{11} and d_{20} can only be determined to within 0.1 Å for oriented bilayers, the errors, which are due mostly to uncertainties in s_1 and c_1, are strongly correlated and the error in the ratio d_{11}/d_{20} is at the 0.1% level which propagates an error of only 0.02° in θ_{tilt}. The main error in θ_{tilt} is in judging the center of the 11 arcs.

Fig. 7 shows x-ray scattering from oriented lipids when the incidence angle ω is large. The six scattering arcs are the expected pattern when the hydrocarbon chains are tilted toward nearest neighbors (12, 41). This film was measured to obtain the angles of the centers of the arcs,

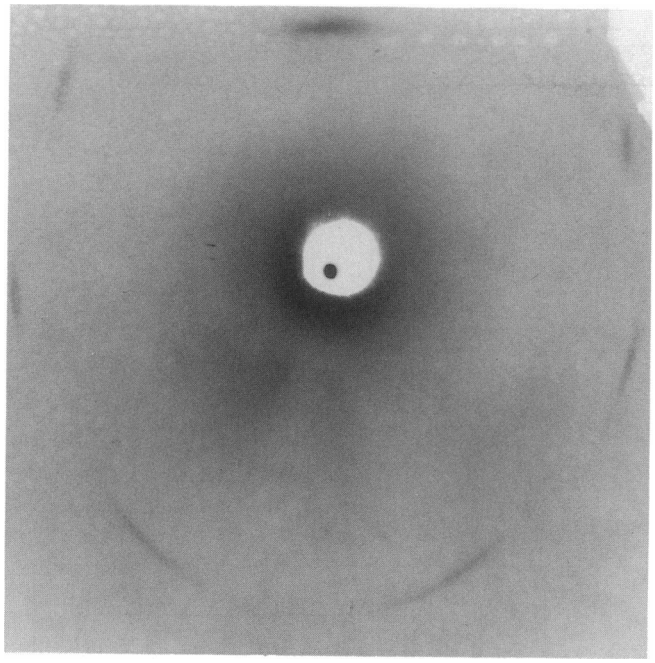

FIGURE 7 Diffraction pattern from oriented bilayers of gel phase $DC_{16}PC$ taken at large angle of incidence, $\omega = 45°$, hydrated at H1 conditions. The dark spot near the center top of the figure is scattering from the mylar windows. The lipid chain packing reflections are indexed as $(\pm 1, 1)$ for the two symmetrical upper arcs, $(\pm 2, 0)$ for the two reflections slightly below the equator and $(\pm 1, -1)$ for the lowest two reflections, which are the longest ones on the films. See Fig. 5 for comparison.

η_{ij}, as well as estimates of the ends of each arc. A computer program was written to fit the chain tilt angle θ, the sample tilt angle ω and the effective chain length L to the data, using Eqs. 4 and 5. Although measuring the ends of each arc is somewhat uncertain, it is clear that the effective chain length L is much closer to 40 Å than to 20 Å. The fitted ω is $45 \pm 1°$, very close to the nominal value set by the 45° wedge used to position the sample holder. The tilt angle θ_{tilt} was consistently about a degree lower than we obtained from the $\omega = 5°$ configuration; this is caused by the differential stretching of the arcs in transforming from q-space to the x-ray film. The most apparent effect of this stretching is the relative elongation of the $(\pm 1, -1)$ arcs, which are elongated more at the lower end than the upper end. This shifts the maximum intensity observed on the film to smaller angles η. Correcting for this removes the discrepancy in θ_{tilt} compared to the $\omega = 5°$ data. Often the *H2* hydrated oriented lipid slid down the coverslip when it was turned to $\omega = 45°$ and the x-ray film was rather light, so our primary determinations of θ_{tilt} for the *H2* sample came from the $\omega = 5°$ data. The six-arc pattern illustrated in Fig. 5 and shown in Fig. 7, is the only type that we observed for either *H1* or *H2* hydration conditions when $\omega = 45°$. In contrast, for unhydrated oriented bilayers θ_{tilt} was effectively zero as evidenced by the appearance of only one pair of arcs in the same position as the 20 arcs seen in Fig. 7, but with arc lengths roughly twice as long (data not shown), corresponding to $L = 20$ Å.

X-ray data from conventional unoriented MLVs are shown in Fig. 8. The experimental configuration caused some slit smearing (7) that shifted low angle rings to lower angles. The two unknowns, D_0 (true spacing) and the coefficient K of the slit smearing shift, $\delta(2\theta) = K \cot an (2\theta)$, were found by the best fit to the observed peaks. Slit smearing was small for $h = 3$ (effecting a perturbation in D of ~0.1 Å) and was insignificant in the wide angle region. The D spacings so obtained are shown in Fig. 9. We were concerned that the $D = 63.4$ Å obtained for $DC_{16}PC$ was somewhat smaller than the $D = 63.7$ Å value that we had obtained previously (48). In an independent set of more careful measurements with superior resolution and negligible slit smearing we confirmed $D = 63.4 \pm 0.1$ Å for $DC_{16}PC$, so we believe that the values shown in Fig. 9 are correct.

The wide angle data shown as insets in Fig. 8 have one sharp peak, corresponding to the 20 reflection, and a broad peak, corresponding to the 11 reflections. The effective area per chain A_c was obtained using Eq. 3 and the values of d_{11} and d_{20} obtained from the Bragg angles of these two peaks. Fig. 10 plots A_c and also θ_{tilt} as a function of chain length. An odd-even effect, typical of hydrocarbon chains, is noticeable in Fig. 10, although the errors are nearly as large as the effect.

From A_c and θ_{tilt}, the area A per lipid is obtained using Eq. 2 with results shown in Table 1. Table 1 also shows n_w, the number of waters per lipid, using Eq. 1. This calculation also requires the lipid volume V_L in $Å^3$/molecule which is obtained using

$$V_L = M_w v (10^{24}/N_A), \quad (6)$$

where M_w is the molecular weight, N_A is Avogadro's number, and v is the specific volume obtained by neutral density centrifugation shown as a function of chain length n in Fig. 11. The results in Table 1 show that the aqueous interface in the gel phase, characterized by A and n_w, remains virtually the same for saturated lecithins with different chain lengths.

DISCUSSION

$DC_{16}PC$

Based on the lamellar D spacing value and the intensity variation between orders, full hydration of ~1,000 oriented bilayers on a solid substrate was achieved under the *H2* hydration conditions. The lamellar D spacing determined from the small ω data for $DC_{16}PC$ was 63.4 ± 0.3 Å which is the same as the value $D = 63.4 \pm 0.1$ Å that was obtained from the usual fully hydrated unoriented MLV dispersion. In addition, the characteristic pattern of lamellar intensities, with the $h = 6$ and $h = 8$ orders absent, was also obtained for our oriented bilayers. No unexplained differences in the diffraction

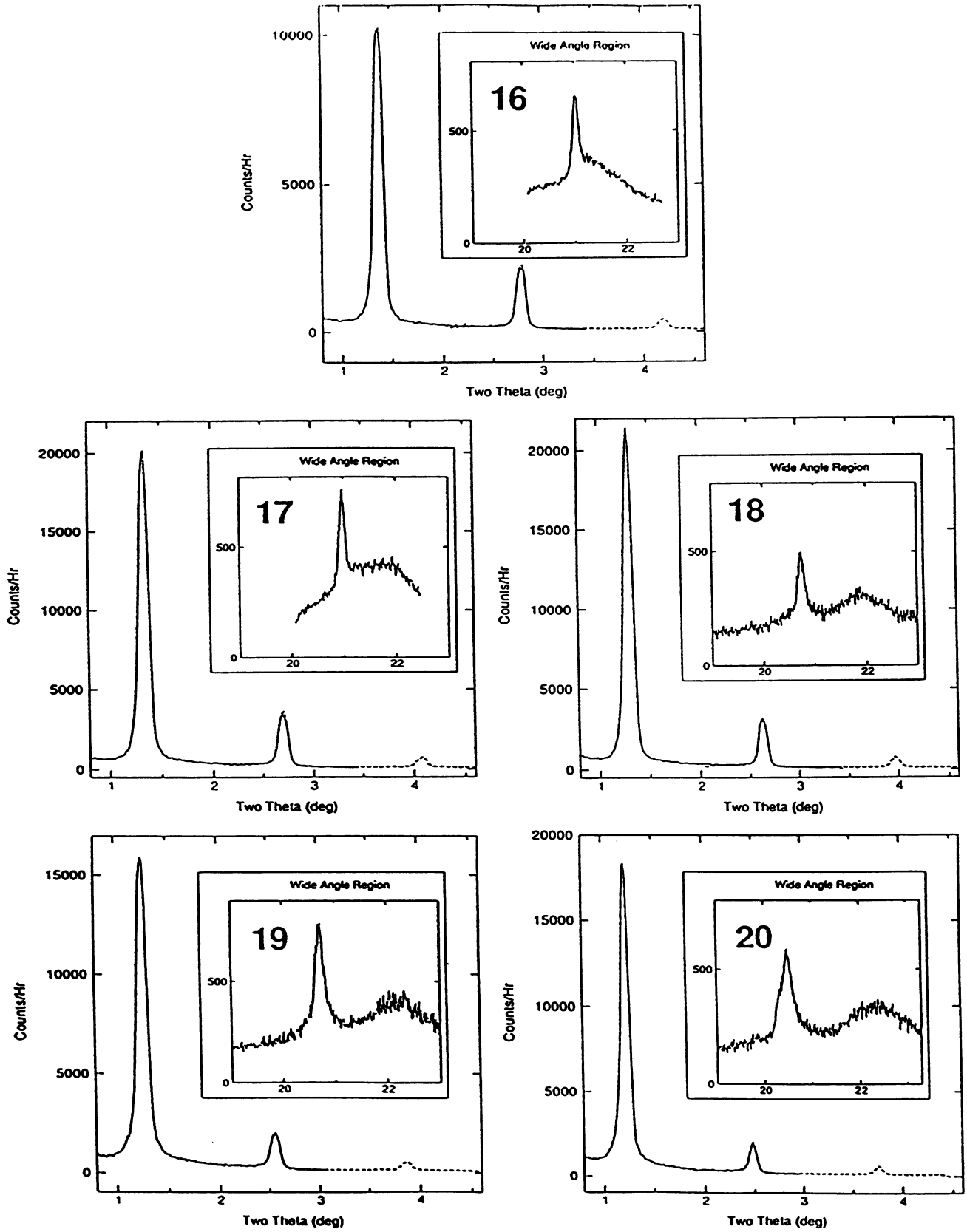

FIGURE 8 Low angle (h = 1, 2, 3) and wide angle (insets) x-ray data taken with the position sensitive detector from fully hydrated unoriented MLVs for DC_nPC for n = 16–20 at T = 19 ± 1°C. The low angle data are divided into two sets, indicated by solid lines and dashed lines, corresponding to two different positions of the PSD. The number in the inset identifies the number of carbon atoms/chain.

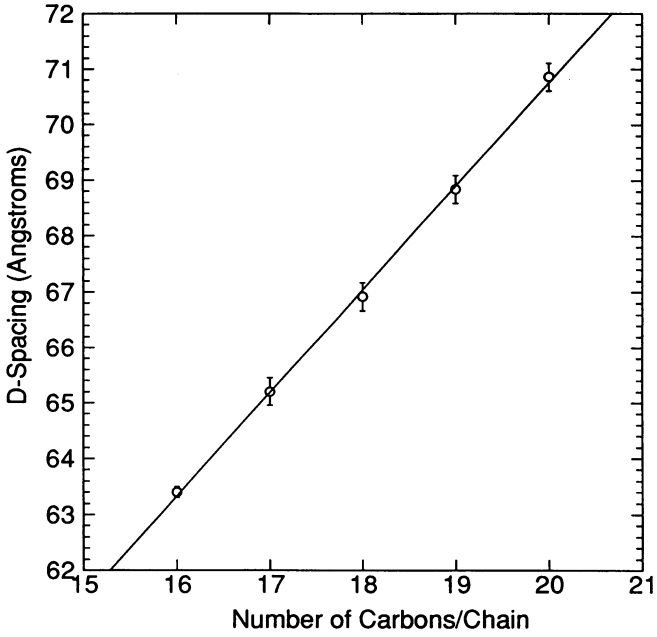

FIGURE 9 Lamellar d-spacings obtained from the low angle x-ray data shown in Fig. 8. Estimated errors take into account slit smearing and instrumental resolution.

patterns of the oriented and unoriented bilayers were observed. This may be contrasted with studies of free standing films where D was 6 Å smaller than for full hydration (40).

The wide angle data taken for $\omega = 45°$ proves the usual picture of chain tilting towards nearest neighbors for *H1* hydration. Although the $\omega = 45°$ data for *H2* hydration

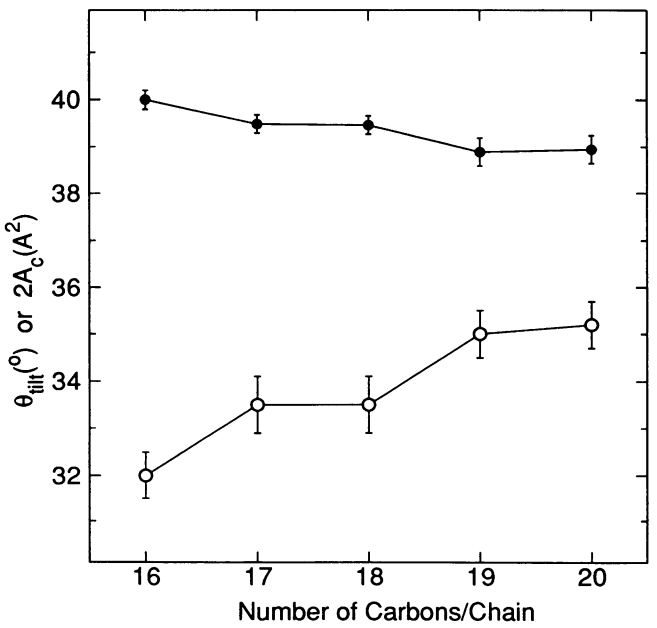

FIGURE 10 Tilt angle θ_{tilt} (*open circles*) and area/chain A_c (*filled circles*) as a function of chain length. $T = 19 \pm 1°C$.

TABLE 1 **Invariance of n_w and A with increasing n**

n	n_w	A (Å^2)
16	11.8 ± 0.7	47.2 ± 0.5
17	11.9 ± 0.8	47.3 ± 0.6
18	11.7 ± 0.8	47.3 ± 0.6
19	11.8 ± 0.9	47.5 ± 0.6
20	11.9 ± 1.0	47.6 ± 0.7

Waters of hydration n_w and area/lipid A as a function of hydrocarbon chain length n.

are sparser due to sliding of the sample off the substrate and poorer due to broadening of the arcs caused by disorder, the $\omega = 5°$ data indicate no change in the position of the visible wide angle arcs for fully hydrated *H2* compared to *H1* hydration. Even *H1* provides nearly full hydration with $D = 62.5$ Å and only faint 6th and 8th orders.

Calculation of θ_{tilt} from the 5° data for *H2* and *H1* and from the 45° data for *H1* all give the same values. For $DC_{16}PC$ our $\theta_{tilt} = 32°$ (at 19°C) is somewhat larger than the values given by or deduced from the work of previous workers. However, the value of $\theta_{tilt} = 30°$ obtained from free-standing films was for $DC_{14}PC$ and this might be expected to be somewhat smaller than for $DC_{16}PC$ due to the trend in θ_{tilt} with chain length n (see Fig. 10); the agreement is therefore satisfactory despite the small D in free-standing films. Also, when McIntosh (24) calculated $\theta_{tilt} = 30°$, he assumed that the DPPC headgroup was also tilted relative to DPPE. If it is assumed that only the chains tilt, then his result would have been $\theta_{tilt} = 31°$, in good agreement with our result.

Our result that θ_{tilt} for dried samples is effectively zero in contrast to $\theta_{tilt} = 32°$ for the fully hydrated $DC_{16}PC$ sample agrees with the result of Levine (20) who con-

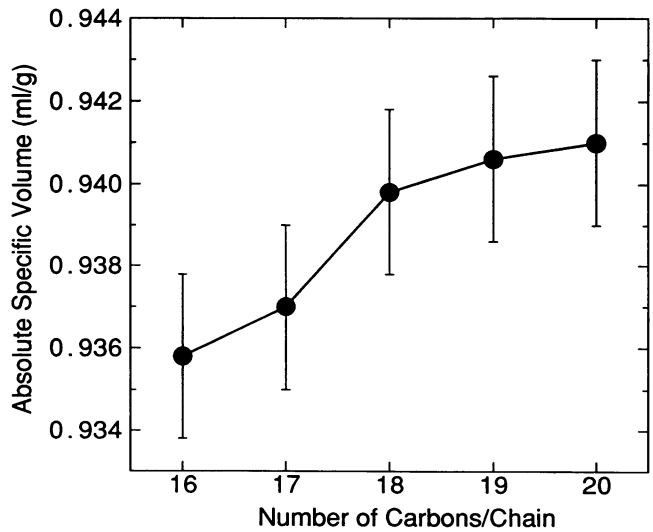

FIGURE 11 Specific volume versus n, number of carbons/chain, measured by neutral density centrifugation (49). $T = 19 \pm 0.2°C$.

cluded that θ_{tilt} increases continuously from 0 for dry lipid up to 28° for 15% water (7.2 water molecules/lipid and D = 59 Å). Our result is also consistent with a recent study of Katsaras and Stinson (18). Although they did not measure θ_{tilt}, their measured headgroup distances $X_{H\text{-}H}$ varied from about 46 Å for their more hydrated sample with D = 60.2 Å to $X_{H\text{-}H}$ = 51.5 Å for their drier sample with D = 58.0 Å. This change in $X_{H\text{-}H}$ is consistent with a decrease in θ_{tilt} to nearly 0°. Also, their $X_{H\text{-}H}$ is nearly the same as the 45 Å previously obtained in this laboratory (48) when D = 63.7 Å.

Our result that θ_{tilt} does not appear to change between fully hydrated *H2* samples and the slightly dehydrated *H1* samples is consistent with there being a threshold dehydration level such that dehydration down to this level does not change bilayer structure. In one *H1* sample of DPPC that was subsequently partially dehydrated, θ_{tilt} was determined to be 32° with D = 58.7 ± 0.4 Å at 19°C. This result is consistent with those of Levine (20) who concluded that there was no change in θ_{tilt} from 15% water to full hydration, which he obtained at 20% water (n_w = 10.2 and D = 64.2 Å). It is also consistent with results of McIntosh and Simon (26) who found that D can be decreased as far as 57.8 Å with little change in the head-head spacing as determined by Fourier electron density profiles using five orders of lamellar diffraction.

Fig. 1 emphasizes that all the values of waters of hydration n_w measured by the gravimetric method are larger than all the values of n_w obtained from all other determinations of θ_{tilt}. This has suggested a systemic reason that meaningful n_w may not be obtainable using the gravimetric/hydration method (30, 48). Unoriented bilayer samples must necessarily have regions with geometric defects that do not give lamellar diffraction; the center of an MLV is just one obvious example. Such regions are probably water-rich compared to the well oriented part of the sample that causes sharp lamellar diffraction. Since the gravimetric method weighs any extra water in the defect regions, it would tend to overestimate n_w. This is an important consideration because nearly all determinations of A and n_w for fully hydrated L_α phases have used the gravimetric/hydration method. If only gravimetric/hydration data are available, then this suggests that the smallest value of n_w should be given preference and that any future gravimetric measurements of n_w should concentrate on lengthy annealing to reduce defect regions.

Further comparisons of the data reviewed in Fig. 1 are somewhat complicated. Fig. 1 shows that there is reasonable agreement between our value of n_w = 11.8 ± 0.7, derived from our measurement of θ_{tilt} for $DC_{16}PC$, and the two earliest determinations of n_w = 13.6 by Tardieu et al. (43) and Janiak et al. (17). However, our value of θ_{tilt} = 33.5° for $DC_{18}PC$ is significantly lower than the range 38–40° obtained by Tardieu et al. (43). This earlier study (43) also concluded that the tilt angle decreased and the bilayer thickness increased continuously with dehydration in contrast to our results and those of McIntosh and Simon (26) and those of Levine (20).

There might be a chronological trend, with n_w increasing with time, and also, by comparing Levine's result (20) with ours, with θ_{tilt} increasing with time. It has been noted that hydrocarbon chain heterogeneity tends to decrease θ_{tilt} (14, 43), so an explanation of the trend would be increasing lipid purity and the good agreement between our results and the early n_w results would then be fortuitous. However, there is no clear chronological trend in lipid purity discernible from many of the primary papers, nor do enough of the gravimetric/hydration papers report enough detail concerning their procedures to suggest any relevant systematic reasons to explain the differences.

While our preparation conditions for orienting samples introduce trace amounts of lysolecithin (~0.1%) into otherwise very pure lipids that give sharp melting transitions (see Materials section), we feel that these trace impurities are not important for the following reason. Prior to hydrating lipid samples using a temperature differential, nearly full hydration of dried lipid was achieved after holding the sample in the hydration chamber for 2 d at 90°C. During this time more lysolecithin (~2%) was formed as determined by thin layer chromatography. Nevertheless, tilt angles for $DC_{16}PC$, $DC_{17}PC$ and $DC_{18}PC$ were the same as when <0.1% lysolecithin was present, demonstrating that a small degree of hydrolysis of the lipid does not affect θ_{tilt}. Also, we have been able to confirm the same tilt angle in ordinary unoriented samples of $DC_{16}PC$. These studies require considerably different kinds of experiments and theory, so they will be reported in a separate paper.

One of the oldest ways to obtain A and bilayer thickness involved plotting D versus $c/(1-c)$ where c is the water concentration (4, 20). For DPPC Levine (20) obtained A = 44.5 $Å^2$ from the range 15% < c < 20%. His analysis required the lipid specific volume to be 1.11 g/ml, which is somewhat larger than our measured value of 1.068 g/ml. It is interesting that, for continuously swelling D,L-DPPC Chapman et al. (4) obtained A = 48 $Å^2$ and θ_{tilt} = 32°, in strikingly good agreement with our present results for L-α-$DC_{16}PC$.

Whatever the explanation for the existing disagreements or agreements in Fig. 1, our present measurements are inconsistent with the large values of area/lipid A obtained from the later gravimetric/hydration measurements and that have become commonly accepted in the literature (32).

Monolayer registry

From the length of the arcs in the data shown in Fig. 7 and the theory in Fig. 5 the length L of the scattering unit along the bilayer normal was estimated to be near 40 Å, twice the length of a single hydrocarbon chain. Since the principal artifact, mosaic spread, lengthens these arcs, our estimate for L is a lower bound. Earlier results on

free-standing films (41) also give values of L that require that the chains from both monolayers in the bilayers be in register. One way that this could come about follows from the inequivalence of the two chains per lipid, with the 1-chain effectively longer than the 2-chain. If the chains are all-*trans*, then efficient packing would require the meeting of 1-chains from one monolayer with 2-chains from the opposing monolayer; this partially interdigitated structure (15, 37, 38) would bring about registry. An alternative model of terminal methyl packing (28), suggested by Raman studies (8), is that the ends of the 1-chain are conformationally disordered. This would allow the 1-chains to bend over near the middle of the bilayer so that they could more nearly match the effective length of the 2-chains. Such a model would, however, present a smoother hydrocarbon surface on each monolayer at the center of the bilayer and would lead one to expect that the monolayers could more easily slide over one another. The x-ray observation that registry exists would therefore seem to favor partial interdigitation. It may also be noted that the length of the apparently single arcs for the dried bilayers was about twice as long as for hydrated bilayers, consistent with the scattering unit being unregistered single monolayers, as was originally suggested by Tardieu et al. (43) when comparing the L_β phase with the $L_{\beta'}$ phase.

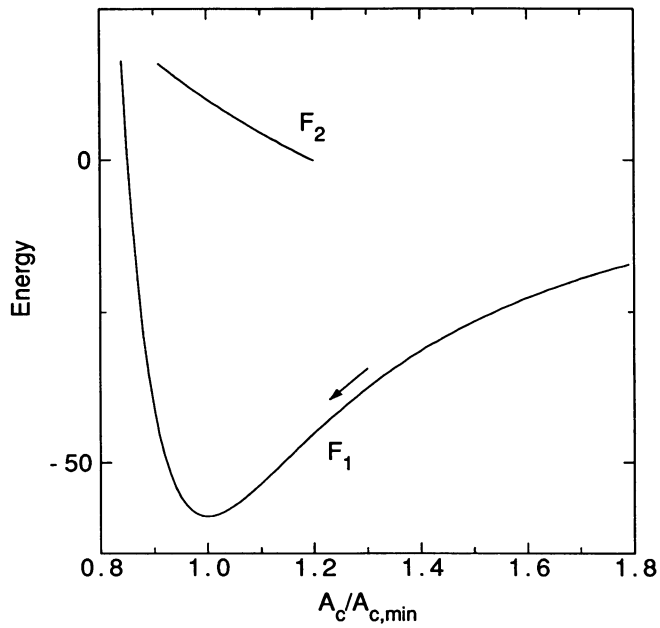

FIGURE 12 Free energy diagram for chain length dependence of θ_{tilt} and A_c. F_1 represents the bulk free energy per methylene and F_2 represents a competing energy discussed in the text. The arrow shows the direction of the minimum for increasing chain length n.

Chain length dependence

Let us now turn our attention to the dependence of DC_nPC structure upon the chain length n. Chains with n shorter than 16 were excluded in this study because their gel phases occur at lower temperatures. We also excluded n larger than 20 because the wide angle patterns appear to be different for n = 22 and 24. Even the data for $DC_{20}PC$ indicate the beginning of a new regime as can be seen by the relatively broad 20 peak in Fig. 8 and the suggestion that there may be a break in the odd-even staircase trend for specific volume in Fig. 11.

The most remarkable feature of our data is that A and n_w are virtually independent of n as seen in Table 1. Quantities that do depend upon n are θ_{tilt} and A_c as seen in Fig. 10. Both θ_{tilt} and A_c exhibit a small odd-even effect; this is characteristic of hydrocarbon chain systems. More important, in our opinion, is an overall increase in θ_{tilt} and decrease in A_c as n increases.

Before attempting to explain the details of the n-dependence, it is first useful to review the reason originally given (24, 27) to explain why chains tilt, namely that tilting allows nearly optimal packing of both the heads and the chains simultaneously. From crystal studies (39), all-*trans* hydrocarbon chains occupy an excluded area of ~19 Å^2. If the chains were pulled apart further than A_c, then there would be a net attractive interaction due to van der Waals forces. With thermal vibration and the introduction of the chain orientational disorder that accompanies melting of crystalline or subgel phases into the gel phase, the chain area expands compared to the area that would apply to crystals at 0 K. Taking these considerations into account suggests a free energy curve per methylene group as a function of A_c, F_1 shown in Fig. 12, with a minimum at a value of $A_{c,min}$ in the vicinity of the values observed for gel phase lipids. In contrast, phosphatidylcholine headgroups require an excluded area considerably larger than the value of $2A_{c,min}$ in Fig. 12. If all-*trans* chains were to hang perpendicularly to the bilayer, then A_c would have to equal $A/2$ = 23.7 Å^2, which would force the chains to climb the energy curve to the right in Fig. 12; this increase in energy can be estimated by the methods of (29, 31) to be ~14 kcal/mol which is even larger than the enthalpy of the main transition (31). A similar perspective is that $\theta_{tilt} = 0°$ and A_c = 23.7 Å^2 would require a volume expansion, when compared to tilted chains, even larger than the volume expansion for the main chain melting transition. There is, therefore, a great deal of energy to drive tilting.

The easiest hypothesis to explain the result that A is constant as n varies is to suppose that the headgroups are pushed together to the point where hard-core, excluded volume repulsive forces dominate. Because repulsive potentials rise steeply, any perturbations, such as those caused by increases in chain length n, that attempt to compress the headgroups further, would bring about only negligible changes in A. A caveat should be noted, however. Tilted fatty acid monolayers can be compressed hard enough to remove the chain tilt (6) and even gel phase $DC_{16}PC$ monolayers can be compressed (13) somewhat below our putative hard-core excluded area of 47.2 Å^2. We believe, however, that substantial

decreases in A would require significant restructuring of the aqueous interface that would likely only begin at an energy threshold considerably higher than the energies involved in changing n from 16 to 20. This is consistent with our observation of the existence of a dehydration threshold for changes in θ_{tilt}. This leads back to the simple picture that a minimum headgroup volume determines θ_{tilt}.

The n dependence of θ_{tilt} and A_c shown in Fig. 10 are now strongly coupled by Eq. 2 because A is constant. This n dependence can be explained with the aid of the two free energies shown in Fig. 12. The first is the free energy per methylene F_1, which we now specify more precisely as the free energy per methylene that would be obtained in the limit of infinitely long chains at 20°C. The second free energy, F_2, accounts for "end" corrections, due to the finite n. The total free energy F is then

$$F = nF_1 + F_2. \quad (7)$$

As n increases, F is minimized at an equilibrium value of A_c that approaches $A_{c,min}$, the location of the minimum of F_1. In order for the minimum value of F to occur at values of A_c larger than $A_{c,min}$, F_2 must decrease, as drawn in Fig. 12, with increasing A_c and decreasing θ_{tilt}, at least for values of θ_{tilt} in the range 30–35°.

Let us identify possible sources for the F_2 free energy. First, there may be a free energy cost to tilting the chains at the headgroup end of the lipid molecule, such as at a conformational hinge or even tilting of the headgroup. Second, the packing free energy associated with the terminal methyl end of the chains may depend upon θ_{tilt}. Only the latter source can give rise to the small odd-even effect observed in Fig. 10, so it may be presumed that this contributes to F_2, though this by no means eliminates other sources. A third source derives from the loss of van der Waals cohesive energy near a surface. Use of the second order correction term in Eq. 8 of Hawton and Keeler (10) yields the F_2, with a constant subtracted, plotted in the graph in Fig. 12. Another datum that may be considered is that A_c for DLPE, 20.6 Å^2 (25), is larger than for any of the longer chain DC$_n$PC. This datum is consistent with the latter two sources of energy because DLPE has a shorter chain length ($n = 12$) but it is inconsistent with the hinge effect because the zero tilt in DLPE is smaller than for the PCs.

Although the chain length dependence of gel phase structure is a rather small effect, it is important to emphasize that it occurs. If the contrary assumption is made that θ_{tilt}, as well as A and n_w, does not depend on n, then a simple, but erroneous, procedure for obtaining θ_{tilt} is to equate the easily measured increase in D to the extra length per methylene, (1.27 Å) cos (θ_{tilt}), of additional methylenes. With the data in Fig. 9 this procedure yields $\theta_{tilt} = 44°$ for all chain lengths. This value of θ_{tilt} is consistent with the largest values of n_w measured by the gravimetric/hydration method. However, the results in this paper show that both are quite incorrect, because θ_{tilt} does indeed have a significant chain length dependence.

We wish to thank Dr. David Rhodes for suggesting measurement at two film distances when ω is small, Drs. Steve Garoff and Frances Separovic for helpful discussions about orienting lipid films, and Greg Rhodes for helping with the specific volume measurements.

This research was supported by grant GM-44976 from the National Institutes of Health.

Received for publication 16 July and in final form 30 October 1992.

REFERENCES

1. Blazyk, J. F., D. L. Melchior, and J. M. Steim. 1975. An automated differential scanning dilatometer. *Anal. Biochem.* 68:586–599.
2. Buldt, G., H. U. Gally, J. Seelig, and G. Zaccai. 1979. Neutron diffraction studies on phosphatidylcholine model membranes. II. Chain conformation and segmental disorder. *J. Mol. Biol.* 134:693–706.
3. Buldt, G., H. U. Gally, J. Seelig, and G. Zaccai. 1979. Neutron diffraction studies on phosphatidylcholine model membranes. I. Head group conformation. *J. Mol. Biol.* 134:673–706.
4. Chapman, D., R. M. Williams, and B. D. Ladbrooke. 1967. Physical studies of phospholipids. *Chem. Phys. Lipids.* 1:445–475.
5. Cornell, B. A., and F. Separovic. 1983. Membrane thickness and acyl chain length. *Biochem. Biophys. Acta.* 733:189–193.
6. Lin, B., M. C. Shih, T. M. Bohanon, G. E. Ice, and P. Dutta. 1990. Phase diagram of a lipid monolayer on the surface of water. *Phys. Rev. Lett.* 65:191–194.
7. Eastabrook, J. N. 1952. Effect of vertical divergence on the displacement and breadth of x-ray powder diffraction lines. *Brit. J. Appl. Phys.* 3:349–352.
8. Gaber, B. P., and W. L. Peticolas. 1977. On the quantitative interpretation of biomembrane structure by raman spectroscopy. *Biochim. Biophys. Acta.* 465:260–274.
9. Harlos, K. 1978. Pretransitions in the hydrocarbon chains of phosphatidylethanolamines. *Biochim. Biophys. Acta.* 511:348–355.
10. Hawton, M. H., and W. J. Keeler. 1986. van der Waals energy of lecithins in the ripple phase. *Phys. Rev. A.* 33:3333–3340.
11. Hentschel, M., and R. Hosemann. 1983. Small- and wide angle x-ray scattering of oriented lecithin multilayers. *Mol. Cryst. Liq. Cryst.* 94:291–316.
12. Hentschel, M. P., and F. Rustichelli. 1991. Structure of the ripple phase $P_{\beta'}$ in hydrated phosphatidylcholine multimembranes. *Phys. Rev. Lett.* 66:903–906.
13. Hifeda, Y. F., and G. W. Rayfield. 1992. Evidence for first-order phase transitions in lipid and fatty acid monolayers. *Langmuir.* 8:197–200.
14. Hui, S. W. 1976. The tilting of the hydrocarbon chains in a single bilayer of phospholipid. *Chem. Phys. Lipids.* 16:9–18.
15. Hui, S. W., and C.-H. Huang. 1986. X-ray diffraction evidence for fully interdigitated bilayers of 1-stearoyllysophosphatidylcholine. *Biochemistry.* 25:1330–1335.
16. Inoko, Y., and T. Mitsui. 1978. Structural parameters of DPPC. *J. Phys. Soc. Japan.* 44:1918–1924.
17. Janiak, M. J., D. M. Small, and G. G. Shipley. 1976. Nature of the thermal pretransition of synthetic phospholipids: dimyristoyl- and dipalmitoyllecithin. *Biochemistry.* 15:4575–4580.
18. Katsaras, J., and R. H. Stinson. 1990. High-resolution electron

density profiles reveal influence of fatty acids on bilayer structure. *Biophys. J.* 57:649–655.

19. Laggner, P., K. Lohner, G. Degovics, K. Muller, and A. Schuster. 1987. Structure and thermodynamics of the DHPC-water system. *Chem. Phys. Lipids.* 44:31–60.
20. Levine, Y. K. 1970. X-Ray Diffraction Studies of Membranes. Thesis, University of London. 1:1–114.
21. Levine, Y. K. 1973. X-ray diffraction studies of membranes. *Prog. Surface Sci.* 3:279–352.
22. Lis, L. J., M. McAlister, N. Fuller, R. P. Rand, and V. A. Parsegian. 1982. Interactions between neutral phospholipid bilayer membranes. *Biophys. J.* 37:657.
23. Luzzati, V. 1967. X-ray diffraction studies of lipid-water systems. *In* Biological Membranes. D. Chapman, editor. Academic Press, London. 71–123.
24. McIntosh, T. J. 1980. Difference in hydrocarbon chain tilt between hydrated PEs and PCs. *Biophys. J.* 29:237–245.
25. McIntosh, T. J., and S. A. Simon. 1986. Area per molecule and distribution of water in fully hydrated dilauroylphosphatidylethanolamine bilayers. *Biochemistry.* 25:4948–4952.
26. McIntosh, T. J., and S. A. Simon. 1986. Hydration force and bilayer deformation: a reevaluation. *Biochemistry.* 25:4058–4066.
27. Nagle, J. F. 1976. Theory of lipid monolayer and bilayer phase transition: effect of headgroup interactions. *J. Membr. Biol.* 27:233–250.
28. Nagle, J. F. 1980. Theory of the main lipid bilayer phase transition. *Annu. Rev. Phys. Chem.* 31:157–195.
29. Nagle, J. F., and M. Goldstein. 1985. Decomposition of entropy and enthalpy for the melting transition of polyethylene. *Macromolecules.* 18:2643–2652.
30. Nagle, J. F., and M. C. Wiener. 1988. Structure of fully hydrated bilayer dispersions. *Biochim. Biophys. Acta.* 942:1–10.
31. Nagle, J. F., and D. A. Wilkinson. 1978. Lecithin bilayers: density measurements and molecular interactions. *Biophys. J.* 23:159–175.
32. Parsegian, V. A. 1983. Dimensions of the intermediate phase of DPPC. *Biophys. J.* 44:413–415.
33. Rand, R. P., and V. A. Parsegian. 1989. Hydration forces between phospholipid bilayers. *Biochim. Biophys. Acta.* 988:351–376.
34. Ruocco, M. J., and G. G. Shipley. 1982. Characterization of the sub-transition of hydrated DPPC bilayers; kinetic, hydration and structural study. *Biochem. Biophys. Acta.* 691:309–320.
35. Seddon, J. M., G. Cevc, R. D. Kaye, and D. Marsh. 1984. X-ray diffraction study of the polymorphism of hydrated diacyl- and dialkylphosphatidylethanolamines. *Biochemistry.* 23:2634–2644.
36. Seddon, J. M., K. Harlos, and D. Marsh. 1983. X-ray diffraction study of the polymorphism of hydrated diacyl- and dialkylphosphatidylethanolamines. *J. Biol. Chem.* 258:3850–3854.
37. Serrallach, E. N., G. H. deHaas, and G. G. Shipley. 1984. Structure and Thermotropic Properties of Mixed-Chain Phosphatidylcholine Bilayer Membranes. *Biochemistry.* 23:713–720.
38. Sisk, R., Z. Wang, H. Lin, and C. Huang. 1990. Mixing behavior of identical molecular weight phosphatidylcholines with various chain-length differences in two-component lamellae. *Biophys. J.* 58:777–783.
39. Small, D. M. 1986. The Physical Chemistry of Lipids, Handbook of Lipid Research. Plenum Press, New York. 672 pp.
40. Smith, G. S., C. R. Safinya, D. Roux, and N. A. Clark. 1987. X-ray study of freely suspended films of DMPC. *Mol. Cryst. Liq. Cryst.* 144:235–255.
41. Smith, G. S., E. B. Sirota, C. R. Safinya, and N. A. Clark. 1988. Structure of the L_β phases in DMPC. *Phys. Rev. Lett.* 60:813–816.
42. Stamatoff, J. B., W. F. Graddick, L. Powers, and D. E. Moncton. 1979. Direct observation of the hydrocarbon chain tilt angle in phospholipid bilayers. *Biophys. J.* 25:253–261.
43. Tardieu, A., V. Luzzati, and F. C. Reman. 1973. Structure and polymorphism of the hydrocarbon chains of lipids: a study of lecithin-water phases. *J. Mol. Biol.* 75:711–733.
44. Thurmond, R. L., S. W. Dodd, and M. F. Brown. 1991. Molecular areas of phospholipids as determined by ^2H NMR spectroscopy. *Biophys. J.* 59:108–113.
45. Torbet, J., and M. H. F. Wilkins. 1976. X-ray diffraction studies of lecithin bilayers. *J. Theor. Biol.* 62:447–458.
46. Tristram-Nagle, S., Zhang, and J. F. Nagle. 1991. X-ray diffraction of fully hydrated oriented bilayers of gel phase DPPC. *Biophys. J.* 59:500*a*. (Abstr.)
47. White, S. H., R. E. Jacobs, and G. I. King. 1987. Partial specific volumes of lipid and water in mixtures of egg lecithin and water. *Biophys. J.* 52:663–665.
48. Wiener, M. C., R. M. Suter, and J. F. Nagle. 1989. Structure of the Fully Hydrated Gel Phase of DPPC. *Biophys. J.* 55:315–325.
49. Wiener, M. C., S. Tristram-Nagle, D. A. Wilkinson, L. E. Campbell, and J. F. Nagle. 1988. Specific volumes of lipids in fully hydrated bilayer dispersions. *Biochim. Biophys. Acta.* 938:135–142.